

AD-A175 977

RADIATION THRESHOLD LEVELS FOR NOISE DEGRADATION OF

1/1

PHOTODIODES. (U) AEROSPACE CORP EL SEGUNDO CA

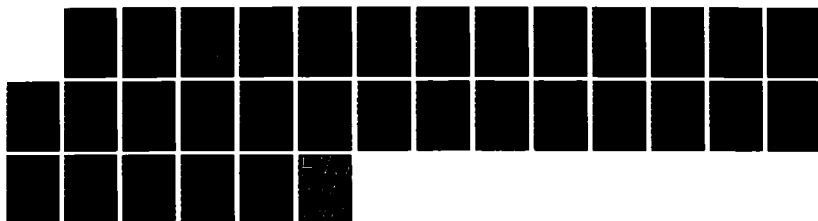
ELECTRONICS RESEARCH LAB L W HUKERMAN ET AL 30 SEP 86

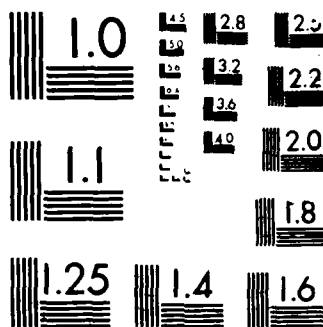
UNCLASSIFIED

TR-0086(6925-04)-2 SD-TR-86-82

F/G 9/1

NL





AD-A175 977

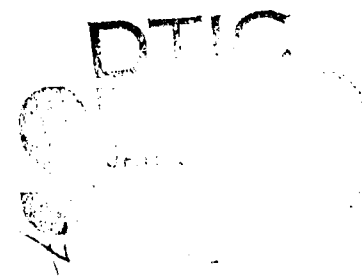
Radiation Threshold Levels for Noise Degradation of Photodiodes

L. W. AUKERMAN, F. L. VERNON, Jr., and Y. SONG
Electronics Research Laboratory
Laboratory Operations
The Aerospace Corporation
El Segundo, CA 90245

30 September 1986

Prepared for
SPACE DIVISION
AIR FORCE SYSTEMS COMMAND
Los Angeles Air Force Station
P.O. Box 92960, Worldway Postal Center
Los Angeles, CA 90009-2960

APPROVED FOR PUBLIC RELEASE:
DISTRIBUTION UNLIMITED



UNCLASSIFIED

SECURITY CLASSIFICATION OF THIS PAGE (When Data Entered)

REPORT DOCUMENTATION PAGE		READ INSTRUCTIONS BEFORE COMPLETING FORM
1. REPORT NUMBER SD-TR-86-82	2. GOVT ACCESSION NO.	3. RECIPIENT'S CATALOG NUMBER
4. TITLE (and Subtitle) RADIATION THRESHOLD LEVELS FOR NOISE DEGRADATION OF PHOTODIODES		5. TYPE OF REPORT & PERIOD COVERED
		6. PERFORMING ORG. REPORT NUMBER TR-0086(6925-04)-2
7. AUTHOR(s) Lee W. Aukerman, Frank L. Vernon, Jr., and Yeong Song		8. CONTRACT OR GRANT NUMBER(s) F04701-85-C-0086
9. PERFORMING ORGANIZATION NAME AND ADDRESS The Aerospace Corporation El Segundo, CA 90245		10. PROGRAM ELEMENT, PROJECT, TASK AREA & WORK UNIT NUMBERS
11. CONTROLLING OFFICE NAME AND ADDRESS Space Division Los Angeles Air Force Station Los Angeles, CA 90009-2960		12. REPORT DATE 30 September 1986
		13. NUMBER OF PAGES 36
14. MONITORING AGENCY NAME & ADDRESS (if different from Controlling Office)		15. SECURITY CLASS. (of this report) Unclassified
		15a. DECLASSIFICATION/DOWNGRADING SCHEDULE
16. DISTRIBUTION STATEMENT (of this Report) Approved for public release; distribution unlimited.		
17. DISTRIBUTION STATEMENT (of the abstract entered in Block 20, if different from Report)		
18. SUPPLEMENTARY NOTES		
19. KEY WORDS (Continue on reverse side if necessary and identify by block number) Noise Photodiodes Radiation effects Space radiation		
20. ABSTRACT (Continue on reverse side if necessary and identify by block number) Space radiation can increase the noise of photodiodes as a result of either a sustained ionizing dose rate effect or displacement damage. Elementary, straightforward models are presented for calculating radiation threshold levels and "rad hit" susceptibility. Radiation-effects experiments that verify these models are discussed. Calculations for room-temperature silicon p-i-n photodetectors, an avalanche photodiode, and a hypothetical cooled staring detector indicate that this damage mechanism should not be ignored for space and nuclear environments.		

DTIC
SERIALIZED
JAN 15 1987
E

DD FORM 1473
FACS MILEUNCLASSIFIED
SECURITY CLASSIFICATION OF THIS PAGE (When Data Entered)

CONTENTS

I.	INTRODUCTION.....	5
II.	THE RADIATION ENVIRONMENT.....	7
III.	NOISE IN PHOTODIODES.....	9
IV.	THE CONTINUOUSLY IONIZING RADIATION ENVIRONMENT.....	17
V.	RADIATION HITS.....	19
VI.	DISPLACEMENT DAMAGE AND TOTAL IONIZING DOSE (TID).....	21
VII.	NUMERICAL EXAMPLES AND CONCLUSIONS.....	29
	REFERENCES.....	35

FIGURES

1.	Cross Section of a More-or-Less Typical n^+/p Photodiode with Guard Ring.....	10
2.	Geometry for Calculating the Number of Electronic Charges per Event.....	12
3.	RMS Noise Voltage Spectrum for a p^+/n Photodiode Obtained from United Detector Technology, before and after Exposure to 1.2×10^{15} electrons cm^2 at 2 MeV.....	23
4.	Plots of the Mean-Square Noise Voltage vs. Dark Current for Two Irradiated Photodiodes.....	24
5.	The Experimental Data for (Dark Current)/(Active Volume) vs. Neutron Fluence.....	26

TABLES

1.	Photodiode Characteristics and Radiation Response.....	30
2.	Material Properties.....	31
3.	Parameters of Hypothetical $Hg_{1-x}Cd_xTe$ Photodiode at 200 K.....	33



Accession For	
NTIS GRA&I	<input checked="" type="checkbox"/>
DTIC TAB	<input type="checkbox"/>
Unannounced	<input type="checkbox"/>
Justification	
By _____	
Distribution/	
Availability Codes	
Dist	_____ / or _____
A-1	

I. INTRODUCTION

Space systems employ photodiodes in many applications, such as optical communications, fiber optics, star sensors, and staring sensor arrays. The effects of space radiation environments on electronic circuits has been well documented in the literature; however, little work of this nature has been carried out on photodiodes. Space radiation can decrease the responsivity and increase the noise of photodiodes. The decrease in responsivity is probably a relatively minor problem if the device is fully depleted and utilizes a properly designed guard ring.¹ On the other hand, if it is operating in a radiation environment, the increase in noise due to an increase in dark current resulting from either displacement damage or a sustained ionizing dose rate may compromise the noise-equivalent power (NEP) or D^* of the device.

Osburn et al.² and Mitchell³ have suggested figures of merit to compare the hardness of various photodiodes to ionizing radiation. In each case the figure of merit considered was proportional to the normalized ratio of the optical photocurrent to the radiation-induced increase in current. Such a figure of merit is useful for comparing photodetectors within a given type, but can give a misleading result when comparing a p-i-n with an avalanche photodiode, for example. One must also keep in mind the fact that such a figure of merit says nothing about the unirradiated sensitivity of a device; otherwise, in eagerly improving the indicated hardness, one could end up with a dead detector.

In this report we calculate the threshold doses and dose rates and review, where appropriate, published radiation-effects work on photodiodes, in order to justify these calculations. Two different applications are considered: (1) wide-bandwidth, uncooled, amplifier-noise-limited operation (e.g. for fiber optic or laser communication); and (2) narrow-bandwidth, cooled, and either background- or detector-limited operation, such as would be applicable for staring detector arrays. In the first category both p-i-n and avalanche photodiodes (APD) are included; in the latter, p-i-n or junction diodes are included.

II. THE RADIATION ENVIRONMENT

The radiation environments that are of concern in space electronic applications can be broadly categorized into those of natural and nuclear origins. The components of radiation encountered by a spacecraft vary widely in their relative and absolute magnitudes, depending on the natural environment, the nuclear scenario, and the specific orbit.

In the immediate vicinity of the earth, within the magnetosphere, the natural particle environment consists, for the most part, of cosmic rays, occasional solar flares, and Van Allen (magnetically trapped) radiation.⁴ Cosmic rays can cause soft errors in low-level logic elements and increase the bit error rate in optical detectors in digital communication systems;⁵ however, in some cases a photodiode's bit error rate resulting from high-energy electrons may greatly exceed that resulting from cosmic rays.

The Van Allen radiation consists mostly of energetic electrons and protons trapped in the earth's magnetic field. The fluxes are strongly dependent on energy, position, and time. For protons of energy greater than 10 MeV, the omnidirectional flux in certain regions of space can be as high as 2×10^5 protons $\text{cm}^{-2} \text{sec}^{-1}$; for electrons of energy greater than 1 MeV, the flux can be 2×10^8 electrons $\text{cm}^2 \text{sec}^{-1}$ (Ref. 6). The maximum unshielded dose rate likely to be encountered is about 3 rads(Si) sec^{-1} (Ref. 6). Of course, after an exoatmospheric nuclear event, the trapped radiation fluxes will be considerably enhanced, possibly by orders of magnitude.

The nuclear environment depends upon the scenario one wants to consider. An exoatmospheric nuclear event yields mostly γ rays, x rays, and fast neutrons. Most of this radiation is emitted in a fast pulse about 20 to 50 ns wide. If the spacecraft survives the initial blast of thermal x rays, the primary concern then becomes the effects of the prompt γ rays, the neutrons, and the buildup of the trapped radiation belts that give rise to a sustained radiation dose over a long period of time.

The damage produced in semiconductor devices subjected to these hostile environmental factors can be categorized in terms of ionization damage (a rearrangement of electrical charge) and displacement damage (a physical rearrangement of some of the atoms of a crystal).

III. NOISE IN PHOTODIODES

The major sources of noise in an ideal photodiode are (1) Johnson noise and (2) shot noise. The latter results from the dark current or the dc component of the signal current. Since 1/f noise is relatively unimportant at high frequencies, it will be neglected in this discussion. Radiation will generate additional shot noise terms: Displacement damage produces Shockley-Read recombination/generation centers that increase the dark current; the presence of a sustained dose rate of ionizing radiation or SIDR (sustained ionizing dose rate) generates hole-electron pairs in the depletion region and results in a dark current increase proportional to the dose rate. Total ionizing dose, or TID, affects the passivating oxide on silicon devices and increases the surface component of the dark current. This latter mechanism is not as well understood as the others.

Figure 1 shows a section of a "typical" photodiode with a guard ring; however, individual designs may vary considerably. The width of the depletion region and one minority-carrier diffusion length into the (in this case) p-type bulk define the active thickness of the device. Optical or ionizing radiation absorbed in this region will produce a photocurrent or a radiation-induced current, as the case may be.

High-frequency, wide-bandwidth photodiodes should utilize a depletion width sufficiently wide to absorb most of the optical signal, so that the rather sluggish response of the diffusion region is minimized.⁸ Unfortunately, the diffusion region still contributes to the radiation response in the case of SIDR; therefore, as pointed out by Kalma and Hardwick¹ and Mitchell,³ this contribution to the noise can be eliminated by employing totally depleted designs.

The classical expression for the mean-square shot noise current is

$$\overline{i_n^2} = 2qQIB \quad (1)$$

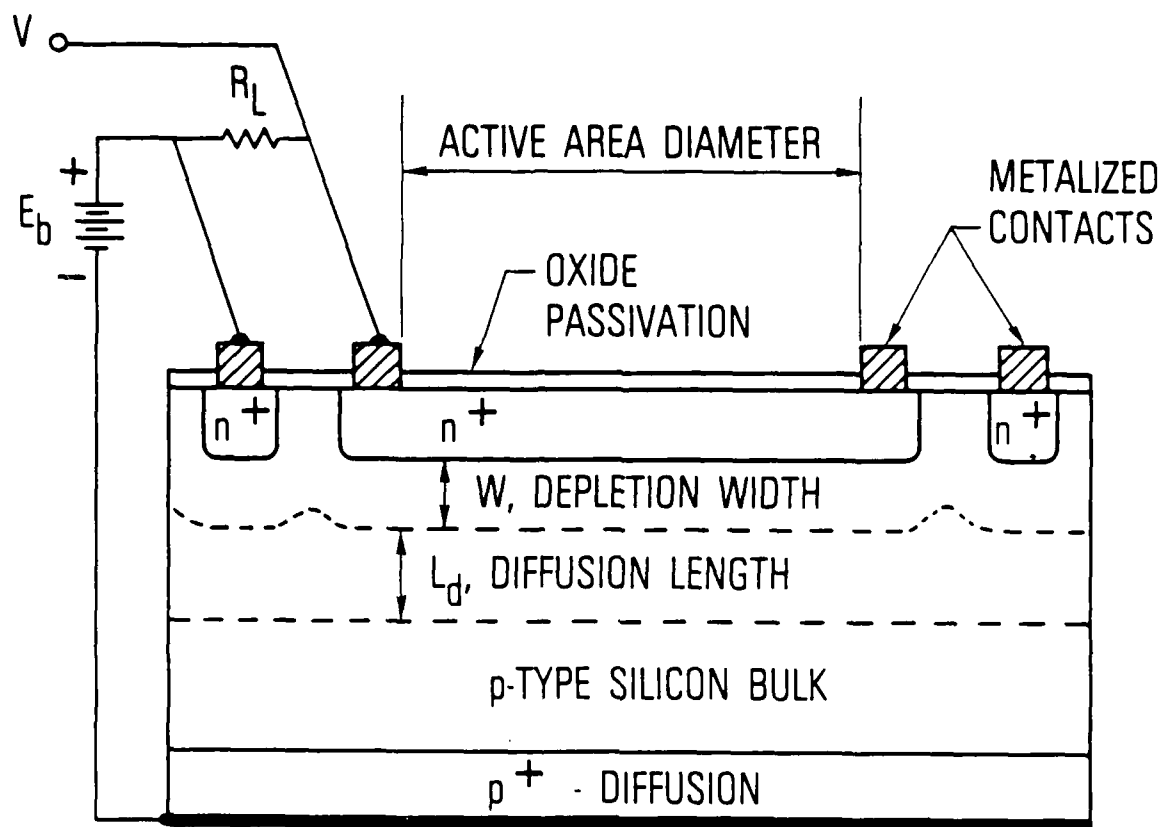


Fig. 1. Cross Section of a More-or-Less Typical n^+/p Photodiode with a Guard Ring

where q is the charge on an electron, Q is the number of electronic charges collected per noise pulse, I is the dc current, and B is the bandwidth. For high-frequency, wide-bandwidth applications, the slow response of the diffusion region does not contribute to the amplitude of the noise pulses if $(1/B) < (\text{response time of the diffusion region})$. In this case Q in Eq. (1) must be interpreted as the charge collected in the depletion region only -- excluding the diffused charge. The dc current is given by

$$I = qQ_T N \quad (2)$$

where N is the average number of events per second. In this case the total charge collected contributes to the dc current; hence, Q_T (the total collected charge per pulse) is used: $Q_T = \left(\frac{L_D}{W}\right)Q$.

If the noise pulses are distributed in amplitude, then Eq. (1) in differential form becomes

$$d \overline{i_n^2} = 2Bq^2 Q^2 N'(Q) dQ \quad (3)$$

where $N'(Q)dQ$ is the number of events/sec in the range Q to $Q + dQ$. Integration gives a more general formulation of Eq. (1):

$$\overline{i_n^2} = 2q \langle Q \rangle IB \quad (4)$$

where $\langle Q \rangle = \overline{Q^2} / \overline{Q}$ by definition.

For ordinary shot noise $Q = 1$. For generation noise Q is uniformly distributed between 0 and 1, making $\langle Q \rangle = 2/3$.⁹ For radiation-induced noise $\langle Q \rangle$ will depend on the type and energy of the ionizing particle and on the chord length distribution. In a space radiation environment, operating with enough shielding to eliminate most of the protons, but not so many as to generate a large bremsstrahlung component, we need consider only energetic (MeV-range) electrons as the ionizing particles. In this case the range of the electron will be much greater than the thickness L of the active region of the diode (see Fig. 2). The quantity N of Eq. (2) becomes $N = A_r \dot{\phi}$, where A_r

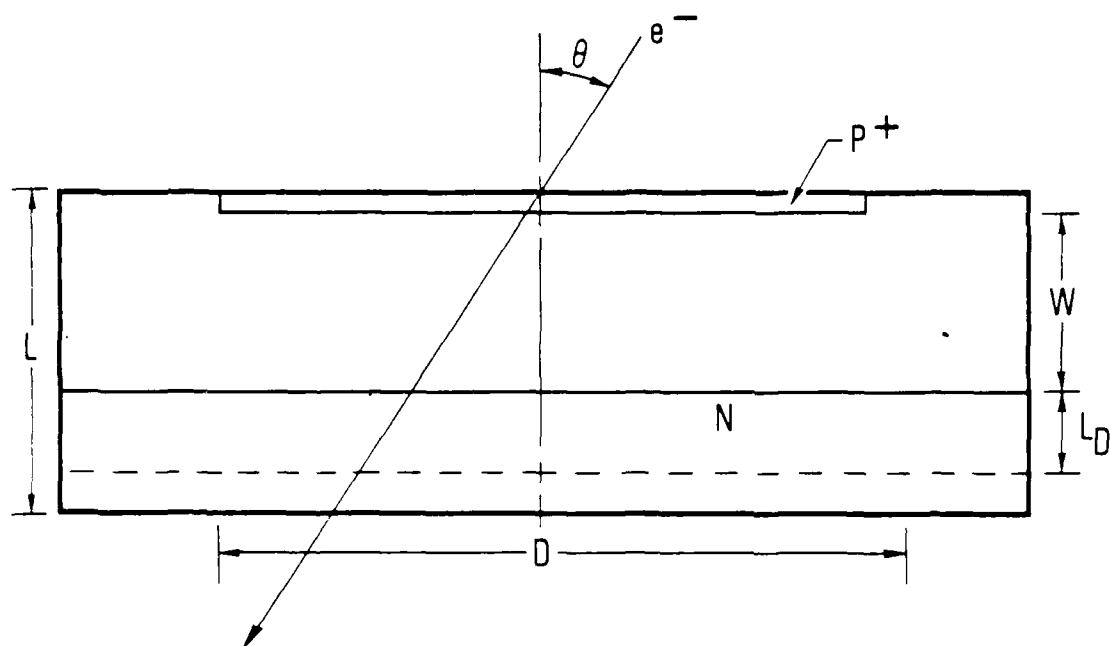


Fig. 2. Geometry for Calculating the Number of Electronic Charges Per Event

is the device area and ϕ is the electron flux ($e \text{ cm}^{-2} \text{ sec}^{-1}$). For $L \ll D$, where D is the diameter of the active region, elementary energy-loss considerations give

$$Q = L(dE/dx)/E_p \cos \theta \quad (5)$$

where dE/dx is the energy lost per unit path length and θ is the angle of incidence (for high-frequency diodes $L = W$). E_p , the average energy required to generate a hole-electron pair, is about 3.7 eV in Si. The distribution in Q will be essentially the chord length distribution [this neglects the stochastic nature of Q in Eq. (5)]. The resulting value for $\langle Q \rangle$ then becomes

$$\langle Q \rangle \approx Q_0 \ln(D/L)/(1 - L/D) \quad (6)$$

for omnidirectional electrons, where Q_0 is the value for Q at normal incidence ($\theta = 0$). Equation (6) also applies to gamma irradiation, where energetic electrons are produced by the Compton and photoelectric effects.

The total mean-square shot noise for a p-i-n or junction photodiode is

$$\overline{i_{ns}^2} = 2q[(2/3)I_{db} + \langle Q \rangle I_r + I_{ds} + I_{bg} + I_s]B \quad (7)$$

where I_{db} , I_r , I_{ds} , I_{bg} , and I_s are the dc currents corresponding respectively to the bulk dark current, dose-rate-induced current (SIDR), the surface dark current, the current due to background radiation, and the optical signal current. For 100% modulation the rms signal current is $i_s = I_s/\sqrt{2}$.

The available signal power is⁸

$$P_{av} = i_s^2/4R_s \omega_0^2 C^2 \quad (8)$$

where R_s is the series resistance and C is the parallel combination of the diode and parasitic capacitance. Eq. (8) is strictly true only at the resonant frequency, ω_0 ; nevertheless, for "low- ω " wideband circuits, such as would likely be used for laser communication or fiber optics, Eq. (8) should be approximately correct for $\omega \ll \omega_0$. The signal-to-noise ratio S becomes

$$S = I_s^2 / 2(\overline{i_{ns}^2} + 4kTB/R_{eq}) \quad (9)$$

The last term in the denominator represents the Johnson noise,⁸ and $R_{eq} = 1/R_s \omega_0^2 C^2$. In a practical photodiode I_s is negligible in comparison to the other current terms in Eq. (7). Then, by solving Eq. (9) for I_s and substituting the usual expression relating I_s to the signal power P_s , or

$$I_s = nqP_s/h\nu \quad (10)$$

we obtain the well-known expression¹⁰ for P_0 , the signal power needed for a signal-to-noise ratio of S:

$$P_0 = (h\nu/qn)(2\overline{Si_n^2}/M^2)^{1/2} \quad (11)$$

(For $S = 1$, P_0 is the noise equivalent power, NEP.) The above expression has been generalized to include the avalanche photodiode (APD) by inserting the current gain M in the denominator. For a p-i-n or p⁺/n photodiode, $M = 1$. In Eq. (11), $\overline{i_n^2}$ is the generalized expression for the total mean-square noise current:

$$\overline{i_n^2} = 2qM^2[(2/3)I_{db}F_d + \langle Q \rangle I_r F_r + I_{bg}F_s]B + 2qI_{ds}B + 4kTFB/R_{eq} \quad (12)$$

The excess noise factors F_d , F_r , and F_s are inserted to take care of the fact that the current multiplication is itself a stochastic process.¹¹ The quantity F is the noise figure of the preamplifier.

For digital modulation the bandwidth would be about equal to one half the maximum bit rate, or approximately $\omega_0/4\pi$. It can be shown that for $B \ll \omega_0/\pi$

$$R_{eq} \approx 1/\pi BC \quad (13)$$

Thus, in the case of a regular p-i-n diode, a high data rate causes the Johnson noise term of Eq. (12) to dominate, but in the case of an APD the shot noise terms become relatively more important and may start to approach the Johnson noise. For this reason APDs are expected to be much more sensitive to radiation effects than are p-i-n devices.

IV. THE CONTINUOUSLY IONIZING RADIATION ENVIRONMENT

A continuously ionizing environment (or SIDR), e.g. the magnetically trapped radiation belts, produces an increase in dark current I_r , according to the well-verified relation^{1,3}

$$I_r = qg_0 A_r L \dot{\gamma} \quad (14)$$

where g_0 is the hole-electron pair generation rate, A_r is the device area, and $\dot{\gamma}$ is the dose rate.

This increases the shot noise according to Eq. (7). Hardwick and Kalma¹² have measured the rms noise of an HP 5082-4207 p-i-n photodiode while it was being irradiated with 1-MeV electrons. Their experimental result for the rms noise current was $i_{rms} = 3.2 \times 10^{-13} (\dot{\phi})^{1/2}$, where $\dot{\phi}$ is the electron flux in $e \text{ cm}^{-2} \text{ sec}^{-1}$. The radiation-induced current was $I_r = 5.2 \times 10^{-10} \dot{\gamma}$, and the active area was $1.2 \times 10^{-2} \text{ cm}^2$. For 1-MeV electrons, $(\dot{\gamma}/\dot{\phi}) = 2.41 \times 10^{-8} \text{ rad cm}^2$. These data can be used to verify Eq. (1). Combining Eqs. (1), (2), and (4), one obtains

$$i_{rms} = qQ_T [2BA_r W / (L_D + W)]^{1/2} (\dot{\phi})^{1/2} \quad (15)$$

$(L_D + W)$ can be determined from Eq. (14) by using $g_0 = 4.04 \times 10^{13} / \text{cm}^3 \text{ rad}$. The depletion width was determined in two ways. From capacitance measurement, $W \approx 23 \text{ } \mu\text{m}$. From the reported quantum efficiency and known absorption coefficient, a value of $21 \text{ } \mu\text{m}$ was calculated for W ; this method of determining W is used throughout this report. Q_T was determined by putting the known value of I_r into Eq. (2) and solving for Q_T . The resulting value for i_{rms} is

$$i_{rms} = 2.8 \times 10^{-13} (\dot{\phi})^{1/2}$$

which yields satisfactory agreement with the experimental value of

$$I_{rms} = 3.2 \times 10^{-13} (\dot{\phi})^{1/2}$$

In a sustained ionizing environment (SIDR) the shot noise due to the radiation induced current I_r will become noticeable when the corresponding shot noise term of Eq. (12) approaches the Johnson, or amplifier, noise. Thus, from Eq. (12) we obtain the following threshold condition:

$$2qM^2[(2/3) I_{db} F_d + \langle Q \rangle I_r F_r + I_{bg} F_s] + 2qI_{ds} = 4kT F/Req \quad (16)$$

For SIDR all shot noise terms are set equal to zero, except the one that relates to the sustained ionization photocurrent, I_r . Then, by incorporating Eq. (14), the threshold level for SIDR is converted into a threshold dose rate $\dot{\gamma}_{ST}$, so that

$$\dot{\gamma}_{ST} = 2\pi kTFBC / (q^2 M^2 F_r g_0 A_r L \langle Q \rangle) \quad (17)$$

For a background or detector-limited photodiode, the threshold condition is taken to be that point at which the SIDR term [the term containing I_r in Eq. (12)] begins to dominate the noise. In this case $\dot{\gamma}_{ST}$ becomes

$$\dot{\gamma}_{ST} = [(2/3) I_{db} + I_{ds} + I_{bg}] / (\langle Q \rangle q g_0 A_r L) \quad (18)$$

In the case of thermal background radiation, the background power incident on the detector can be calculated from the Planck radiation law¹³ to obtain I_{bg} .

V. RADIATION HITS

Another way of looking at the noise resulting from SIDR is to consider whether the individual pulse resulting from the passage of an energetic electron through the active region of a photodiode is large enough to be interpreted by the system as a real signal. These radiation hits, or rad hits, can produce error bits in a data communications system; i.e., they are single-event effects.

If we remove the term $\overline{i_{ns}^2}$ from Eq. (9) and solve for I_s , this quantity is the signal current required for a signal-to-noise ratio of S ; therefore, the ratio R_{rh} of the peak rad hit current ($2\pi BqQ$) to I_s can be useful for determining the susceptibility of a detector to rad hits. R_{rh} is called the rad hit susceptibility ratio since, if $R_{rh} > 1$, the detector is susceptible to rad hits from the angle θ or greater. Combining Eqs. (5) and (9) and incorporating the noise figure F and the current gain M for the avalanche detector, one obtains

$$R_{rh} = qW(dE/dx)M/[E_p(2SkTFC/\pi)^{1/2}\cos\theta] \quad (19)$$

In Eq. (5) the active thickness L was assumed to be the depletion width W , since we are concerned with the fast component of the noise pulse. For a much lower bandwidth, background- or detector-limited sensor, the rad hit susceptibility ratio becomes

$$R_{rh} = [\pi L(dE/dx)/(E_p \cos\theta)](Bq/[S\{(2/3)I_{db} + I_{bg}\}])^{1/2} \quad (20)$$

where, in this case, the active thickness is considered to be the sum of the depletion width and the diffusion length ($L \approx W + L_d$). (dE/dx) is tabulated in Ref. 14.

VI. DISPLACEMENT DAMAGE AND TOTAL IONIZING DOSE (TID)

Displacement damage affects responsivity through carrier removal and mobility lowering, but this is most likely a small effect. However, displacement damage can severely affect minority carrier lifetime and diffusion length. This can quickly decrease responsivity if the depletion width is small enough that optical absorption can occur beyond the depleted region. Kalma and Hardwick, in their radiation study of several commercial photodiodes,¹ found considerable responsivity degradation in nondepleted diodes after about 10^{11} to 10^{12} n cm⁻², whereas the fully depleted devices were fairly hard up to about 10^{13} to 10^{14} n cm⁻². To complete the picture the effect of displacement damage on shot noise should also be considered.

Lattice defects resulting from displacement damage are responsible for deep-level Shockley-Read recombination-generation levels which, in the depletion region, increase the spontaneous rate of electron-hole generation and consequently increase the bulk dark current I_{db} (or generation current).

The dark current resulting from these deep levels is¹⁵ $qWA_r n_i / 2\tau_g$, where n_i is the intrinsic carrier density and τ_g is the generation lifetime (τ_g is related to the electron and hole emission probabilities by the Shockley-Read theory¹⁶). The bulk dark current can be expressed as

$$I_{db} = I_{db_0} + qWA_r n_i \Psi / 2K_g \quad (21)$$

$$1/\tau_g = 1/\tau_{g_0} + \Psi/K_g \quad (22)$$

where Ψ is the fluence (or total dose) and K_g is the appropriate damage constant.

Studies of the noise resulting from generation current are hard to find in the literature. Scott and Strut have verified the 2/3 factor for generation noise in the depletion region.⁹ Bräunig et al. have observed increased NEP, presumably a result of increased generation noise, after irradiation of several commercial photodiodes with 1.5-MeV electrons.¹⁷ Kalma and Hardwick¹

demonstrated an increase in rms noise voltage by almost a factor of ten as a result of a neutron fluence of $10^{14} \text{ n cm}^{-2}$.

Figure 3 shows the noise spectra obtained at The Aerospace Corporation¹⁸ with a p⁺/n photodiode obtained from United Detector Technology. The device had been irradiated with $1.2 \times 10^{15} \text{ electrons cm}^{-2}$ at 2 MeV. The bottom curve shows the preirradiation results, which are Johnson- and amplifier-noise limited. Various load resistors were used, as indicated in the figure, in order to determine the effective shunt resistance R_S of the generation current noise source (R_S is not necessarily the dynamic resistance of the device). For two different samples, EJ1 and EJ2, R_S was $(600 \pm 100) \text{ k}\Omega$ and $(580 \pm 80) \text{ k}\Omega$, respectively.

Figure 4 is a plot of the mean-square noise voltage versus reverse dark current for the above two samples, with $R_L = 105 \text{ k}\Omega$. From the equivalent circuit in the inset,

$$\overline{i_n^2} = \frac{\overline{v_n^2}}{R_S^2} + \frac{\overline{v_n^2}}{R_L^2} \quad (23)$$

and from Eq. (23),

$$\overline{v_n^2} = (4/3)qIB R_S^2 R_L^2 / (R_S^2 + R_L^2) \quad (24)$$

This equation is used to calculate the solid lines of Fig. 4. The dark current is presumed to be bulk generation current because of the large area (0.03 cm^2) and the fact that the temperature dependence of the dark current was consistent with that expected for deep levels in the depletion region. Note that the noise from EJ2 is very accurately predicted by the calculated result. The noise for EJ1 is slightly, but consistently, high. The deviations for this sample seem to occur more frequently at the higher voltages, suggesting possibly a slight tendency for microplasma formation.

From the known increase in dark current and Eq. (21), we obtain, for the 1-MeV electron damage constant, $K_{ge} = 2.7 \times 10^{-13} \text{ sec cm}^{-2}$.

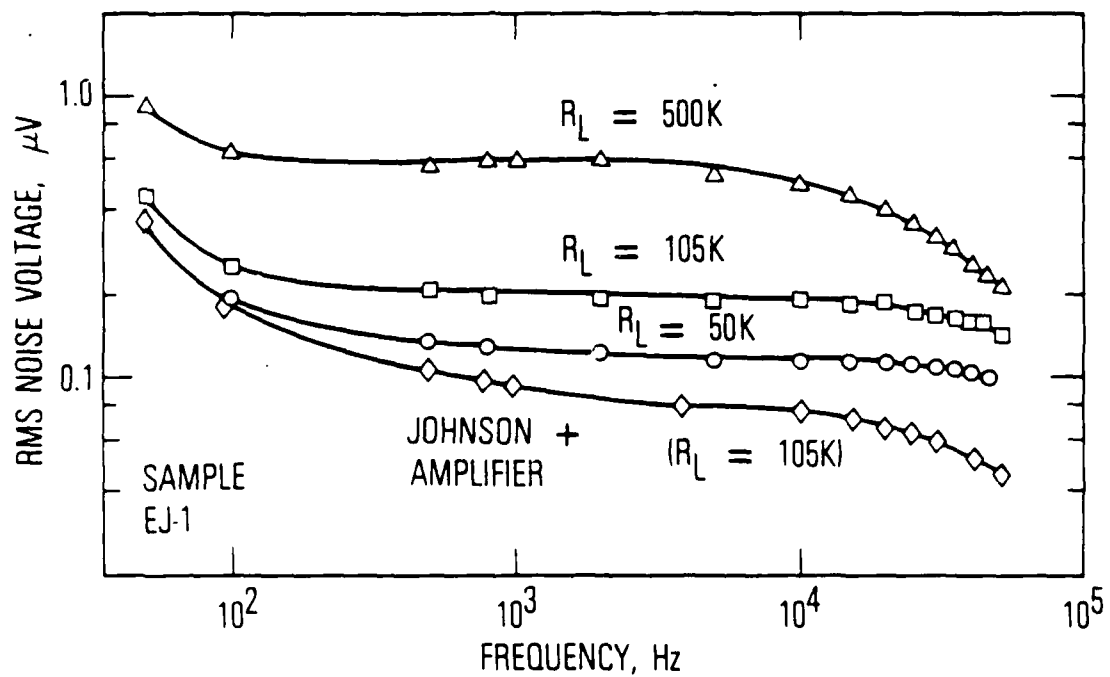


Fig. 3. RMS Noise Voltage Spectrum for a p^+/n Photodiode Obtained from United Detector Technology, before (diamonds) and after Exposure to 1.2×10^{15} Electrons cm^{-2} at 2 MeV. Bandwidth is 6 Hz. R_L = load resistance.

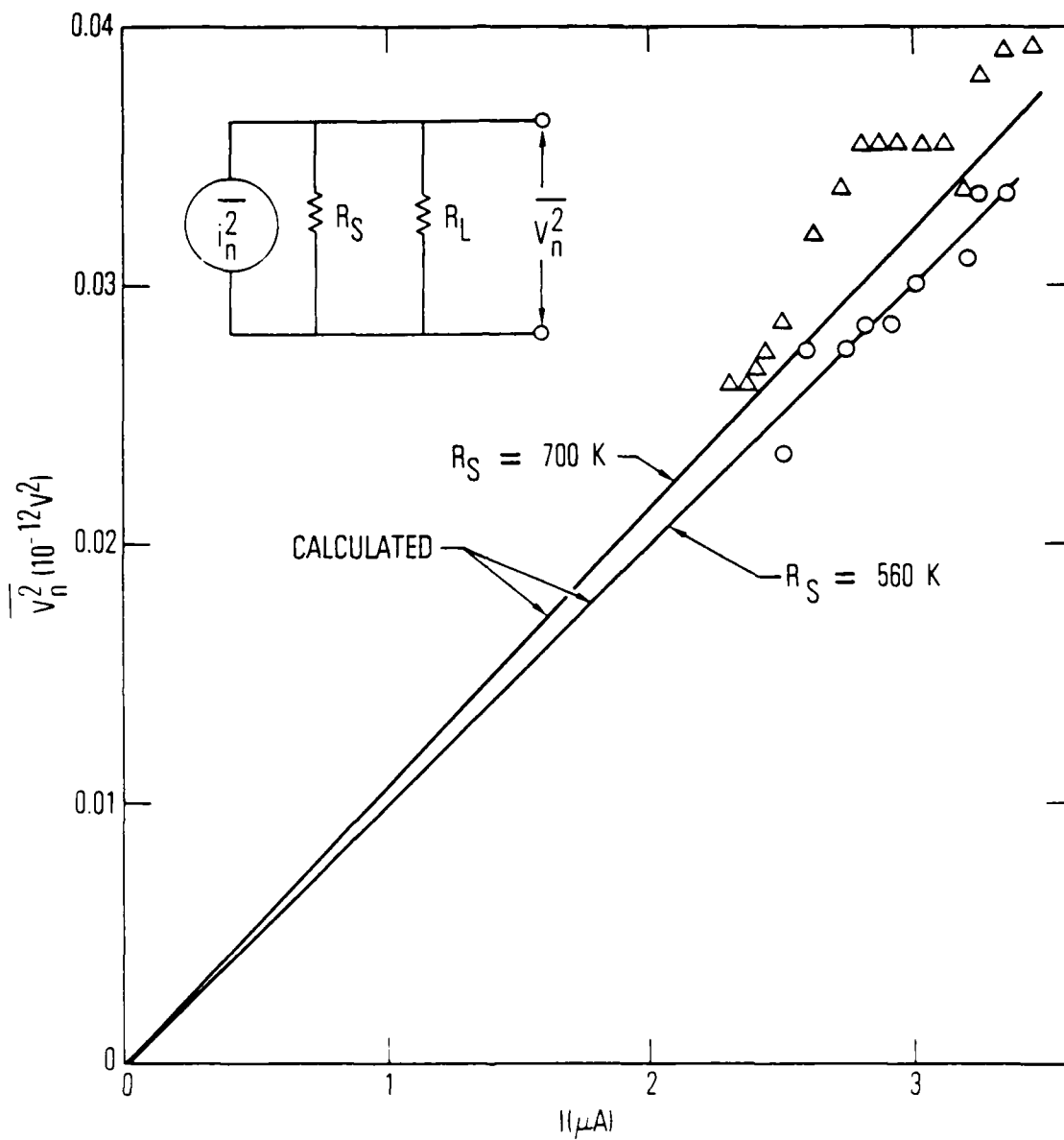


Fig. 4. Plots of the Mean-Square Noise Voltage vs. Dark Current for Two Irradiated Photodiodes. The calculations were made with the Scott-Strutt⁹ 2/3 factor and the indicated shunt resistance values.

The increase in photodiode dark current resulting from neutron irradiation shows considerable scatter and a definite sublinear trend, as indicated in Fig. 5, where the results of Kalma and Hardwick¹ on a large number of commercial devices, and of Barnes¹⁹ on an EG&G YAG 100, lie in the shaded region. A point determined from the results of a study carried out on avalanche detectors²⁰ also lies within the shaded region at $2.4 \times 10^{12} \text{ n cm}^{-2}$, after division by the current gain.

The reason for the sublinear behavior is not well understood. The solid line of Fig. 5 is the calculated result based on Eq. (21) and the value for K_{gn} of 0.7×10^7 obtained by Srour et al. from measurements of the Zerbst effect on MOS capacitors.²¹ This value of K_{gn} fits the data well at low fluence, but overestimates the dark current at high fluence. Invoking surface leakage does not seem to provide a natural explanation for the sublinear behavior.

The dark current increases resulting from gamma irradiation, on the other hand, appear to be dominated by surface effects.¹ Furthermore, the results are so variable and inconsistent that there is no point in trying to establish a damage constant for all samples. In order to determine total ionizing dose (TID) effects on a given device, it will be necessary to rely on empirical results for the particular device under consideration (see Fig. 7 of Ref. 1).

The shot noise threshold fluence Ψ_T for displacement damage is obtained by substituting Eq. (21) for I_{db} in Eq. (16) and neglecting the other shot noise terms. The initial bulk dark current I_{db0} is considered negligible. The results are

$$\Psi_T = 6\pi k T F K_{gBC} / (q^2 M^2 F_d W A_r n_i) \quad (25)$$

for the amplifier-limited case. For the background- or detector-limited case, the threshold condition is satisfied when the radiation-induced increase in bulk dark current [Eq. (21)] is equal to the sum of the other shot-noise-generating currents of Eq. (12), i.e.,

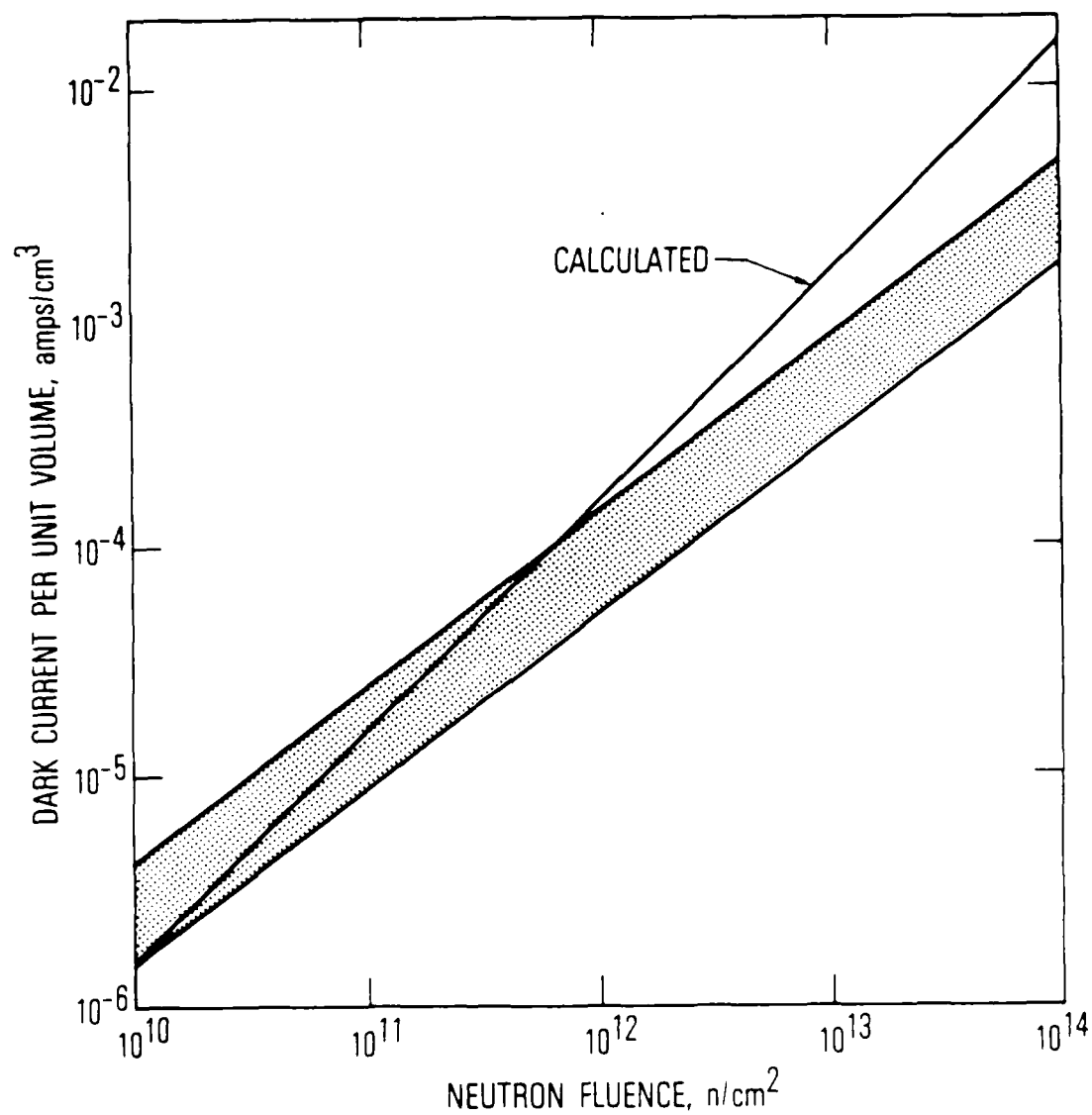


Fig. 5. The Experimental Data (in the shaded region) for (Dark Current)/(Active Volume) vs. Neutron Fluence.^{1,19,20} The calculated line is based on the damage constant of Srour et al.²¹

$$\psi_T = 3[(2/3)I_{db} + I_{ds} + I_{bg}]K_g/(qWA_r n_i) \quad (26)$$

for the background- or detector-limited case.

The total dose effect of ionizing radiation is most likely to increase the surface leakage. Assuming this mechanism for TID, the threshold condition occurs when

$$I_{ds} = 2\pi BCFkT/q \quad (27)$$

and when

$$I_{ds} = M^2 I_{bg} \quad (28)$$

for amplifier-limited and background-limited cases, respectively. The latter two results can be converted into threshold doses with the help of empirically determined dark current versus dose data. The surface dark current increase may be relatively unimportant in the case of APDs, since it is not multiplied by the current gain factor M ; however, there may be other damage mechanisms present that are not considered here, e.g. microplasma formation.¹¹

Equations (17) through (20) and (25) through (28) are useful for designing radiation-hardened detectors or predicting the radiation noise degradation of off-the-shelf items. Equations (17) and (18) should be quite accurate as long as the necessary parameter values can be obtained. The rad hit susceptibility ratio R_{rh} gives a qualitative result. The model used here may be rather simplistic, but it provides useful guidelines nonetheless. The damage constant for generation current K_g is not yet well-defined experimentally, so estimates of displacement-damage noise are presently qualitative. Fortunately, however, this source of noise appears to be no problem for most applications of nonavalanching photodiodes. All calculations made on APDs are qualitative, because of uncertainties in the current gain and, especially, the excess noise factors. Nevertheless, it will be seen that the APDs are so much softer than regular photodiodes that a qualitative result is all that is needed to demonstrate this fact.

VII. NUMERICAL EXAMPLES AND CONCLUSIONS

Calculations of threshold levels for three commercial, Johnson noise/amplifier-limited, commercially available silicon p-i-n photodiodes are listed in Table 1. These are devices that could, conceivably, be considered for an optical communication system, or a fiber optic system. For comparison an APD was also considered. The results, taking 9000 Å for the wavelength, $B = 1$ GHz, and $S = 25$ (corresponding to a bit error probability of about 10^{-7} to 10^{-6}), are also listed. Other parameters needed for the calculations are listed in the top six rows.

The first three columns are for p-i-n diodes, with active volume decreasing from left to right. For the APD, column four, $M = 150$ and $F_r = F_d = F_s = 25$. This is a reasonable value for F_s ,¹¹ but no experimental values could be found for the other excess noise factors, so they were assumed to be about the same as F_s .

Table 1 illustrates the expected decreasing sensitivity to space radiation (increasing threshold, decreasing rad hit susceptibility) as the p-i-n dimensions are reduced. It also indicates a greatly enhanced vulnerability of the APD to sustained ionizing radiation, rad hit susceptibility, and displacement damage, relative to the p-i-n. Note from Eqs. (17) and (25) that increasing the bandwidth decreases the vulnerability to noise degradation, but at the expense of an increased NEP resulting from the increased Johnson noise term. Also, decreasing the depletion width W , especially in a fully depleted device, improves the hardness; but as W approaches or becomes smaller than the reciprocal of the absorption coefficient α , the price paid in terms of increased NEP, resulting from the lower quantum efficiency [see Eq. (11)], becomes prohibitive.^{2,3} Also, increasing α , by going to a shorter wavelength or employing a direct band-gap material, will improve the hardness.² The SPX-3290 was especially designed for radiation hardness, hence the low responsivity. A direct gap material with the same depletion width would have a considerably increased responsivity. At a shorter wavelength (~ 5000 Å) the advantage of a direct gap material would be minimal. Table 2 shows some of the constants used in the calculations.

Table 1. Photodiode Characteristics and Radiation Response

	EG&G YAG 100, p/n	RCA C30807, p/n	Spectronix SPX-3290, n/p	RCA (APD) C30902E
Diameter, mm	2.55	1.0	0.38	0.8
Area, mm ²	5.9	0.87	0.15	0.35
Depletion width, μ m	266	36.5	20	30
Diffusion length, μ m	115	100	7	10
Active volume, mm ²	2.24	0.12	0.004	0.014
Responsivity, A/W (at 9000 Å)	0.62	0.6	0.3	65
A_{rr} , 10 ⁻¹¹ cm ² sec	0.06	0.15	0.38	6.37
Sustained threshold, rad(Si) sec ⁻¹	0.3	15	575	2.3×10^{-4}
\bar{R}_{rh}	9.5	1.3	0.91	270
R_{rh} , $\theta = 0$	5.4	0.74	0.48	142
Displacement threshold, n cm ⁻²	$>10^{16}$	$>10^{16}$	$>10^{16}$	1.5×10^{12}
TID Threshold, rad(Si)	$>10^8$	$>10^8$	$>10^8$	$>10^8$

Table 2. Material Properties (from Ref. 3)

Material	λ , μm	α , cm^{-1}	g_0 , $\text{rad}^{-1} \text{cm}^{-3}$
Si	1.06	35	4.04×10^{13}
	0.9	400	
	0.63	3500	
GaAs	0.63	2.4×10^4	7.16×10^{13}
InP	0.9	1.7×10^4	6.83×10^{13}
GaAs _{0.7} Sb _{0.3}	1.06	1×10^4	1.03×10^{14}

Table 3 shows the results of calculations for a hypothetical, cooled, detector-limited staring detector. The results indicate that for this type of device, shot noise degradation or rad hits cannot necessarily be neglected in an SDR environment.

Table 3. Parameters of Hypothetical $\text{Hg}_{1-x}\text{Cd}_x\text{Te}$ Photodiode at 200 K

$\lambda_{c_0} = 3.75 \text{ } \mu\text{m}, R_0 A_r = 60 \text{ } \Omega \text{ cm}^{-2}, A_r = 10^{-4} \text{ cm}^2$		
$L = 10 \text{ } \mu\text{m}, \text{F.O.V.} < 2 \times 10^{-8} \text{ ster}, g_0 = 5 \times 10^{14} \text{ cm}^{-3} \text{ -rad}$		
$\delta = 7.4 \text{ gm cm}^{-3}, t_r = \frac{1}{2\pi B} = 10^{-3} \text{ sec}$		
SIDR threshold $\dot{\gamma}_{ST} = 0.10 \text{ rad(HgCdTe) sec}^{-1}$		
rad hit susceptibility ratio R_{rh} :		
	$S = 2$	$S = 10$
$\overline{R_{rh}}$	2.6	1.2
$R_{rh} (\theta = 0)$	1.42	0.64

REFERENCES

1. A. H. Kalma and W. H. Hardwick, IEEE Trans. Nucl. Sci. NS-25, 1483 (1978).
2. G. C. Osburn, L. R. Dawson, and J. J. Wiczer, IEEE Trans. Nucl. Sci. NS-28, 4342 (1981); J. J. Wiczer, L. R. Dawson, and C. E. Barnes, IEEE Trans. Nucl. Sci. NS-28, 4397 (1981).
3. K. W. Mitchell, IEEE Trans. Nucl. Sci. NS-24, 2294 (1977).
4. A. L. Vampola, "Radiation Effects on Space Systems and Their Modeling," Space Systems and Their Interactions with Earth's Space Environment, Progress in Astronautics and Aeronautics, No. 171, eds. H. B. Garrett and C. P. Pike (Am. Institute of Aeronautics and Astronautics Publ., New York, 1980), p. 339.
5. J. C. Pickel and J. T. Blandford, IEEE Trans. Nucl. Sci. NS-25, 1166 (1978).
6. L. W. Ricketts, Fundamentals of Nuclear Hardening of Electronic Equipment (Wiley Interscience, New York, 1972).
7. The Trapped Radiation Handbook, DNA 2524H, Defense Nuclear Agency, Washington, D.C. (December 1971).
8. D. H. Seib and L. W. Aukerman, "Photodetectors for the 0.1 to 1.0 μm Spectral Region," Advances in Electronics and Electron Physics, Vol. 34, ed. L. Marton (Academic Press, New York, 1973), p. 169.
9. L. Scott and M. J. O. Strutt, Solid St. Electron. 9, 1067 (1966).
10. K. W. Mitchell, IEEE Trans. Nucl. Sci. NS-25, 1545 (1978).
11. G. E. Stillman and C. M. Wolfe, "Avalanche Photodiodes," Semiconductors and Semimetals, eds. R. K. Willardson and A. C. Beer (Academic Press, New York, 1977), pp. 291-393.
12. W. H. Hardwick and A. H. Kalma, IEEE Trans. Nucl. Sci. NS-26, 4808 (1979).
13. R. H. Kingston, Detection of Optical and Infrared Radiation (Springer-Verlag, New York, 1978).
14. M. J. Berger and S. M. Seltzer, "Tables of Energy Losses and Ranges of Electrons and Positrons," NASA SP-3012, National Aeronautics and Space Administration, Washington, D.C. (1964).

15. A. S. Grove, Physics and Technology of Semiconductor Devices (John Wiley & Sons, Inc., New York, 1967), p. 173.
16. R. N. Hall, Phys. Rev. 87, 387 (1952); W. Shockley and W. T. Read, Phys. Rev. 87, 835 (1952).
17. D. Braüning O. Mienhardt, A. Spenke, and H. G. Wagemann, Ziets. für Angew. Physik 32, 313 (1972).
18. L. W. Aukerman, unpublished results.
19. C. E. Barnes, J. Appl. Phys. 50, 5242 (1979).
20. R. A. Walters and E. C. Hall, Proc. Southeastern 74, Region 3 Conference, Orlando, Fla. (29 April to 1 May 1974) (IEEE, Inc., 1974).
21. J. R. Srour, S. C. Chen, S. Othmer, and R. A. Hartmann, IEEE Trans. Nucl. Sci. NS-25, 1251 (1978); J. R. Srour et al., IEEE Trans. Nucl. Sci. NS-26, 4784 (1979).

END

2-87.

DTIC